European Journal of Medicinal Chemistry 82 (2014) 164–171

Contents lists available at ScienceDirect

European Journal of Medicinal Chemistry

journal homepage: http://www.elsevier.com/locate/ejmech

Original article

New insights into the biological properties of *Crocus sativus* L.: chemical modifications, human monoamine oxidases inhibition and molecular modeling studies

Celeste De Monte [a], Simone Carradori [a, *], Paola Chimenti [a], Daniela Secci [a], Luisa Mannina [a, d], Francesca Alcaro [b], Anél Petzer [c], Clarina I. N'Da [c], Maria Concetta Gidaro [b], Giosuè Costa [b], Stefano Alcaro [b], Jacobus P. Petzer [c, *]

[a] Dipartimento di Chimica e Tecnologie del Farmaco, Sapienza University of Rome, P.le A. Moro 5, 00185 Rome, Italy
[b] Dipartimento di Scienze della Salute, "Magna Graecia" University of Catanzaro, Campus Universitario "S. Venuta", Viale Europa Loc. Germaneto, 88100 Catanzaro, Italy
[c] Pharmaceutical Chemistry and Centre of Excellence for Pharmaceutical Sciences, School of Pharmacy, North-West University, Private Bag X6001, Potchefstroom 2520, South Africa
[d] Istituto di Metodologie Chimiche, Laboratorio di Risonanza Magnetica "Annalaura Segre", CNR, via Salaria km 29.300, 00015 Monterotondo, Rome, Italy

ARTICLE INFO

Article history:
Received 29 January 2014
Received in revised form
13 May 2014
Accepted 21 May 2014
Available online 22 May 2014

Keywords:
Crocin
Crocus sativus L.
hMAO inhibitors
Depression
Neurodegenerative disorders
Safranal

ABSTRACT

Although there are clinical trials and *in vivo* studies in literature regarding the anxiolytic and antidepressant activities of the components of *Crocus sativus* L., their effects on the human monoamine oxidases (hMAO-A and hMAO-B), enzymes which are involved in mental disorders and neurodegenerative diseases, have not yet been investigated. We have thus examined the hMAO inhibitory activities of crocin and safranal (the most important active principles in saffron) and, subsequently, designed a series of safranal derivatives to evaluate which chemical modifications confer enhanced inhibition of the hMAO isoforms. Docking simulations were performed in order to identify key molecular recognitions of these inhibitors with both isoforms of hMAO. In this regard, different mechanisms of action were revealed. This study concludes that safranal and crocin represent useful leads for the discovery of novel hMAO inhibitors for the clinical management of psychiatric and neurodegenerative disorders.

1. Introduction

Traditional herbal medicines have received significant attention for the treatment of specific illnesses, although in many instances limited evidence exist for their mechanisms of action [1]. In particular, a better understanding of the mechanisms of action of these components would greatly facilitate the possibility of discovering new therapeutic agents with fewer side effects, specifically for the treatment of mental and neurodegenerative diseases [2].

Crocus sativus L. (saffron spice) has attracted much attention in the field of medicine, especially with regard to the discovery of psychoactive agents. In fact, chemical analysis of *C. sativus* L. extracts has revealed the presence of more than 150 components in the stigmas such as crocetin (a carotenoid derivative), crocins (diglycosidic esters of crocetin), picrocrocin (responsible for the bitter taste), safranal (the volatile oil responsible for the saffron aroma), anthocyanins, flavonoids, vitamins, amino acids, proteins, starch, mineral substances and gums [3]. With regard to their pharmacological properties, crocin (crocetin di-gentiobiose ester) was found to enhance the memory and learning abilities in ethanol-induced learning behavior impaired mice and rats [4]. Saffron, in turn, was found to be effective in reducing the effects of aluminum-toxicity in adult mice [5]. Components of saffron extracts and crocetin have been shown to bind to the PCP (phenylcyclidine) binding site of the NMDA receptor as well as to the σ1 receptor. Since σ receptor ligands could inhibit the ischemic-induced presynaptic release of excitotoxic amino acids, these saffron extracts may play a role in the management of mental disorders [6].

Moreover, in a double-blind and randomized trial, depressed outpatients were randomly assigned to receive extracts of *C. sativus*

* Corresponding authors.
E-mail addresses: simone.carradori@uniroma1.it (S. Carradori), jacques.petzer@nwu.ac.za (J.P. Petzer).

http://dx.doi.org/10.1016/j.ejmech.2014.05.048
0223-5234/

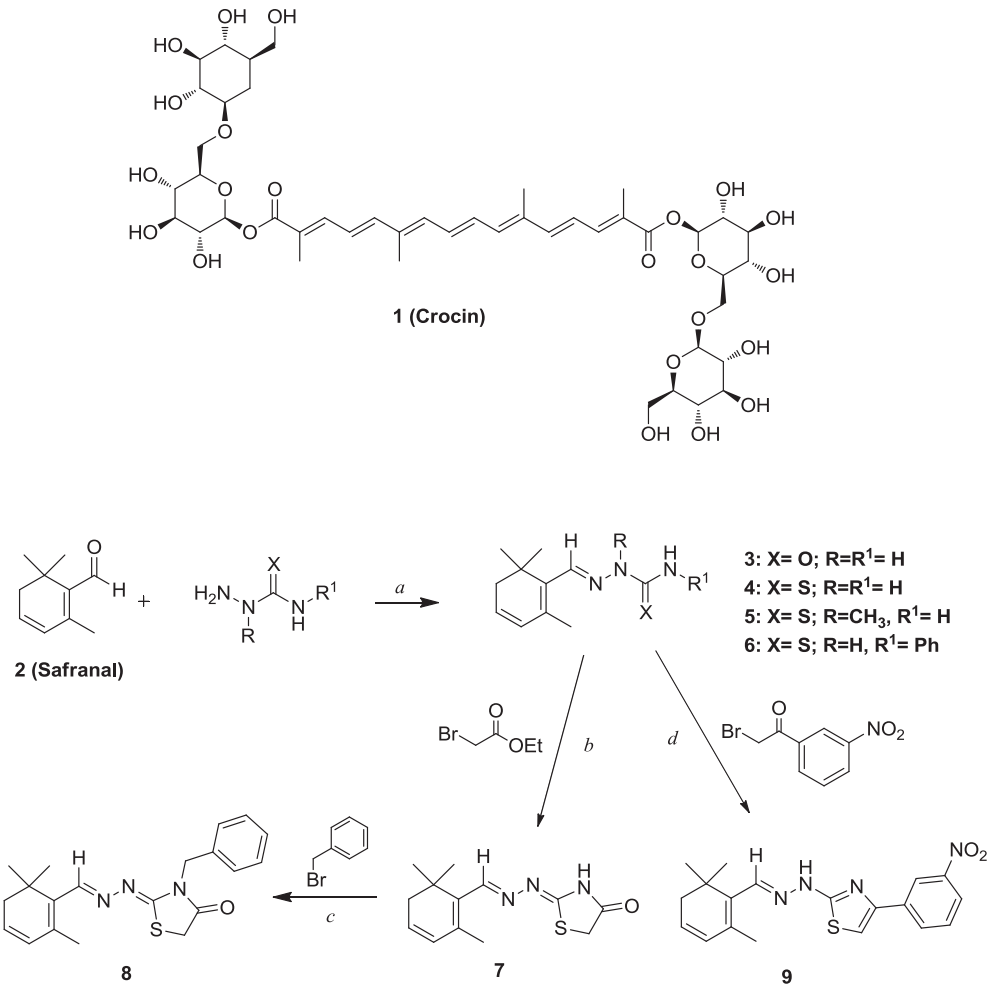

Scheme 1. Structures of bioactive compounds (crocin and safranal) of *Crocus sativus* L. and synthesis of safranal derivatives **3**–**9**. Reagents and conditions: (*a*) EtOH, acetic acid (cat.), rt; (*b*) (if $X = S$ and $R = R^1 = H$) MeOH, CH_3COONa, rt; (*c*) dry acetone, anhydrous K_2CO_3, rt; (*d*) (if $X = S$ and $R = R^1 = H$) EtOH, rt.

L. or fluoxetine and it was found that the efficacies of these treatments are comparable [7]. Similarly, in 6-week double-blind and randomized trials, the effect of a hydro-alcoholic extract of stigmas of *C. sativus* L. was comparable to those of fluoxetine [8] and imipramine [9] in the treatment of mild to moderate depression. Another clinical study that supported the efficacy of saffron active principles as antidepressant agents was a 6-week double-blind, placebo-controlled and randomized trial: at the end of the study patients receiving ethanolic extracts of *C. sativus* L. gave improved outcomes on the Hamilton Depression Rating Scale [10]. It is particularly noteworthy that treatment with saffron extracts is not associated with sexual dysfunction in men and women, a side effect often encountered with antidepressant drugs [11,12]. Evidence suggests that both safranal and crocin contribute to the antidepressant effect of *C. sativus* L. extracts in mice, probably *via* the inhibition of dopamine and norepinephrine re-uptake by crocin, and the inhibition of serotonin reuptake by safranal [13]. Furthermore, saffron and its active constituents provide neuroprotection in a rat model of Parkinson's disease (PD), possess antioxidant effects in an *in vitro* model of Alzheimer's disease (AD), anxiolytic activity in rodents [14] and also neuroprotective effects in animal models of other neurodegenerative conditions such as the retinal dystrophies [15]. The ethanolic extract of saffron stigmas also exhibits antioxidant properties by inhibiting amyloid β-peptide (Aβ) fibril formation and deposition in the human brain, which characterize AD [16]. Even with the limitations of cholinesterase inhibitors, a recent study evaluated new AChE inhibitors which were derived from saffron [17].

Although there are many studies and clinical trials reported in literature regarding the anxiolytic and antidepressant effects of safranal and crocin [2], no detailed pharmacological studies are available to explain the mechanism of action of saffron in the treatment of depression. We are particularly interested in the possibility that saffron components may modulate the activities of the human monoamine oxidase (hMAO) enzymes, which are targets for the treatment of both depression and neurodegeneration. hMAO-A and hMAO-B catalyze the oxidative deamination of endogenous and dietary amines: the hMAO-A isoform is mainly expressed in catecholaminergic neurons and regulates the metabolism of serotonin, epinephrine and norepinephrine, while hMAO-B mostly metabolizes benzylamine and phenethylamine and is expressed in those areas, such as the *substantia nigra*, where dopamine neurons are predominant. Both hMAO isoforms are involved in the metabolism of dopamine [18,19]. The excessive activity of hMAO-A could lead to psychiatric disorders such as depression and dysthymia, while hMAO-B overexpression increases with age and plays a pivotal role in neurodegenerative diseases such as PD and AD [20,21]. Therefore, in our continued interest in the discovery of new leads/scaffolds for the design of hMAO inhibitors [22–25], we first assessed the hMAO inhibitory activities of two main active principles of saffron (Scheme 1): crocin (**1**) and safranal (**2**). These two compounds are characterized by

opposite physicochemical properties, are present in different amounts in the plant, and are usually reported as analytical/pharmacological markers. We also designed and synthesized a new series of safranal derivatives (**3**–**9**, Scheme 1) in order to establish which chemical modifications of the safranal unsaturated nucleus could enhance inhibition potency towards hMAO-A and/or hMAO-B.

2. Materials and methods

2.1. Chemistry

Commercial samples of crocin (crocin-1, crocetin di-gentiobiose ester) and safranal (>88%) were purchased from Sigma–Aldrich (Milan, Italy). Safranal was further purified by column chromatography on silica gel (high purity grade, pore size 60 Å, 230–400 mesh particle size) using ethyl acetate:*n*-hexane (1:3) as the eluant. ^{1}H NMR and IR spectra of the purified product were in agreement with those reported in the literature. The chemicals, solvents for synthesis, and spectral grade solvents were purchased from Sigma–Aldrich and were used without further purification. All melting points were measured on a Stuart® melting point apparatus SMP1, and are uncorrected. ^{1}H and ^{13}C NMR spectra were recorded, respectively, at 400 and 101 MHz on a Bruker spectrometer using $CDCl_3$, CD_3OD and DMSO-d_6 as the solvents. Chemical shifts are expressed as δ units (parts per millions) relative to the solvent signal. Coupling constants *J* are valued in Hertz (Hz). IR spectra were recorded on a FT-IR Perkin–Elmer SpectrumOne equipped with ATR system. Elemental analyses for C, H, and N were recorded on a Perkin–Elmer 240 B microanalyzer and the analytical results were within ±0.4% of the theoretical values for all compounds. All reactions were monitored by TLC performed on 0.2 mm thick silica gel plates (60 F_{254}, Merck).

2.1.1. Bis[(2S,3R,4S,5S,6R)-3,4,5-trihydroxy-6-({[(2R,3R,4S,5S,6R)-3,4,5-trihydroxy-6-(hydroxymethyl)tetrahydro-2H-pyran-2-yl]oxy}methyl)tetrahydro-2H-pyran-2-yl] (2E,4E,6E,8E,10E,12E,14E)-2,6,11,15-tetramethyl-2,4,6,8,10,12,14-hexadecaheptaenedioate (**1**)

Red powder; mp 186 °C; IR: cm^{-1} 3240 (υ O–H), 1694 (υ C=O), 1014 (υ C–O).

2.1.2. 2,6,6-Trimethylcyclohexa-1,3-dienecarbaldehyde (**2**)

Light yellow oil; ^{1}H NMR (400 MHz, CD_3OD): δ 1.19 (s, 6H, 2 × CH_3), 2.16–2.18 (m, 2H, CH_2), 2.19 (s, 3H, CH_3), 5.99–6.03 (m, 1H, CH=), 6.20–6.25 (m, 1H, CH=), 10.12 (s, 1H, CHO); IR (neat): cm^{-1} 2865 and 2749 (υ C–H), 1661 (υC=O). Anal. Calcd. for $C_{10}H_{14}O$: C, 79.96; H, 9.39. Found: C, 79.59; H, 9.01.

2.1.3. 1-((2,6,6-Trimethylcyclohexa-1,3-dienyl)methylene) semicarbazide (**3**)

Semicarbazide hydrochloride (1 eq) was solubilized in the minimum amount of water in presence of sodium acetate (1 eq) and added to a stirring solution of safranal (1 eq) in ethanol (50 mL) at room temperature. After 48 h, the reaction mixture was filtered and the solid was purified by column chromatography (ethyl acetate:*n*-hexane, 1:1) to obtain product **3** as a white powder (mp 170–175 °C, 77% yield); ^{1}H NMR (400 MHz, $CDCl_3$): δ 1.19 (s, 6H, 2 × CH_3), 1.96 (s, 3H, CH_3), 2.15 (s, 2H, CH_2), 5.85–5.94 (m, 2H, 2 × CH=), 6.96 (bs, 1H, NH_2, D_2O exch.), 7.67 (s, 1H, CH=), 7.89 (bs, 1H, NH_2, D_2O exch.), 8.12 (bs, 1H, NH, D_2O exch.); ^{13}C NMR (101 MHz, $CDCl_3$) δ 19.18 (CH_3), 26.90 (2 × CH_3), 33.49 (C), 40.64 (CH_2), 128.27 (CH=), 129.76 (CH=), 133.17 (=CCH_3), 134.51 (C=), 141.69 (C=N), 158.24 (C=O); IR (neat): cm^{-1} 3437 (υ N–H), 1683 (υC=O), 1666 (υC=N). Anal. Calcd. for $C_{11}H_{17}N_3O$: C, 63.74; H, 8.27; N, 20.27. Found: C, 64.02; H, 8.49; N, 20.49.

2.1.4. 1-((2,6,6-Trimethylcyclohexa-1,3-dienyl)methylene) thiosemicarbazide (**4**)

Thiosemicarbazide (1 eq) was added to a stirring solution of safranal (1 eq) in ethanol (50 mL) at room temperature. After 48 h, the reaction mixture was filtered and the solid was washed with *n*-hexane to give product **4** as a yellow powder (mp 188–192 °C, 85% yield); ^{1}H NMR (400 MHz, $CDCl_3$): δ 1.20 (s, 6H, 2 × CH_3), 1.98 (s, 3H, CH_3), 2.16 (s, 2H, CH_2), 5.91 (d, J = 9.6 Hz, 1H, CH=), 5.95–5.99 (m, 1H, CH=), 6.29 (bs, 1H, NH_2, D_2O exch.), 6.95 (bs, 1H, NH_2, D_2O exch.), 7.89 (s, 1H, CH=), 9.51 (bs, 1H, NH, D_2O exch.); ^{13}C NMR (101 MHz, DMSO-d_6) δ 19.38 (CH_3), 27.16 (2 × CH_3), 33.41 (C), 128.99 (CH=), 130.14 (CH=), 133.60 (=CCH_3), 135.61 (C=), 143.95 (C=N), 177.58 (C=S), (CH_2 signal missing due to overlap with DMSO-d_6); IR (neat): cm^{-1} 3427 (υ N–H), 3152 (υ = C–H), 1542 (υC=N), 1289 (υC=S). Anal. Calcd. for $C_{11}H_{17}N_3S$: C, 59.16; H, 7.67; N, 18.81. Found: C, 58.87; H, 7.45; N, 19.07.

2.1.5. 2-Methyl-1-((2,6,6-trimethylcyclohexa-1,3-dienyl) methylene)thiosemicarbazide (**5**)

2-Methylthiosemicarbazide (1 eq) was added to a stirring solution of safranal (1 eq) in ethanol (50 mL) with catalytic amounts of acetic acid at room temperature. After 48 h, the reaction mixture was filtered, the liquid was concentrated *in vacuo* and the obtained solid was filtered and purified by column chromatography (ethyl acetate:light petroleum, 1:2) to give product **5** as a yellow powder (mp 108–110 °C, 77% yield); ^{1}H NMR (400 MHz, DMSO-d_6): δ 1.15 (s, 6H, 2 × CH_3), 1.96 (s, 3H, CH_3), 2.11 (s, 2H, CH_2), 3.72 (s, 3H, CH_3), 5.95 (bs, 2H, 2 × CH=), 7.39 (bs, 1H, NH_2, D_2O exch.), 7.64 (s, 1H, CH=), 8.38 (bs, 1H, NH_2, D_2O exch.); ^{13}C NMR (101 MHz, DMSO-d_6) δ 19.66 (CH_3), 27.10 (2 × CH_3), 32.59 (C), 33.53 (NCH_3), 128.87 (CH=), 130.24 (CH=), 133.59 (=CCH_3), 135.16 (C=), 141.53 (C=N), 180.63 (C=S), (CH_2 signal missing due to overlap with DMSO-d_6); IR (neat): cm^{-1} 3429 (υ N–H), 3235 (υ = C–H), 1571 (υC=N), 1356 (υ C–N). Anal. Calcd. for $C_{12}H_{19}N_3S$: C, 60.72; H, 8.07; N, 17.70. Found: C, 61.03; H, 7.79; N, 18.01.

2.1.6. 1-((2,6,6-Trimethylcyclohexa-1,3-dienyl)methylene)-4-phenylthiosemicarbazide (**6**)

4-Phenylthiosemicarbazide (1 eq) was added to a stirring solution of safranal (1 eq) in ethanol (50 mL) with catalytic amounts of acetic acid at room temperature. After 48 h, the reaction mixture was filtered, the solid was washed with *n*-hexane and light petroleum and purified by column chromatography (ethyl acetate:light petroleum, 1:2) to give product **6** as a yellow powder (mp 161–163 °C, 80% yield); ^{1}H NMR (400 MHz, DMSO-d_6): δ 1.18 (s, 6H, 2 × CH_3), 1.97 (s, 3H, CH_3), 2.11 (s, 2H, CH_2), 5.97 (bs, 2H, 2 × CH=), 7.18 (t, J = 7.2 Hz, 1H, Ar), 7.36 (t, J = 7.8 Hz, 2H, Ar), 7.60 (d, J = 8.4 Hz, 2H, Ar) 8.22 (bs, 1H, NH, D_2O exch.), 9.37 (s, 1H, CH=), 11.54 (bs, 1H, NH, D_2O exch.); ^{13}C NMR (101 MHz, DMSO-d_6) δ 19.63 (CH_3), 27.23 (2 × CH_3), 33.44 (C), 124.68 (CH-benzene), 125.44 (2 × CH-benzene), 128.72 (CH=), 129.36 (CH=), 130.22 (2 × CH-benzene), 133.46 (=CCH_3), 136.24 (C-benzene), 139.28 (C=), 144.42 (C=N), 175.15 (C=S), (CH_2 signal missing due to overlap with DMSO-d_6); IR (neat): cm^{-1} 3306 (υ N–H), 3149 (υ = C–H), 1552 (υC=N), 1195 (υC=S). Anal. Calcd. for $C_{17}H_{21}N_3S$: C, 68.19; H, 7.07; N, 14.03. Found: C, 67.96; H, 7.31; N, 14.29.

2.1.7. 2-(2-((2,6,6-Trimethylcyclohexa-1,3-dienyl)methylene) hydrazono)thiazolidin-4-one (**7**)

The intermediate thiosemicarbazone **4** (1 eq) reacted with ethyl-bromoacetate (1 eq), in methanol (50 mL) and sodium acetate (1 eq) at room temperature under magnetic stirring for 24 h. The reaction mixture was poured on ice, filtered and the solid was washed with light petroleum to give compound **7** as an orange powder (mp 146–151 °C, 81% yield); ^{1}H NMR (400 MHz, DMSO-d_6):

δ 1.15 (s, 6H, 2 × CH_3), 1.94 (s, 3H, CH_3), 2.11 (s, 2H, CH_2), 3.85 (s, 2H, CH_2-thiazolidinone), 5.97–5.98 (m, 2H, 2 × CH=), 8.30 (s, 1H, CH=), 11.87 (bs, 1H, NH, D_2O exch.); ^{13}C NMR (101 MHz, DMSO-d_6) δ 19.22 (CH_3), 27.09 (2 × CH_3), 33.56 (C), 33.67 (CH_2-thiazolidinone) 129.72 (2 × CH=), 130.17 (=CCH_3), 134.16 (C=), 137.08 (C=N), 155.58 (C=N-thiazolidinone), 174.98 (C=O), (CH_2 signal missing due to overlap with DMSO-d_6); IR (neat): cm^{-1} 3448 (υ N–H), 1717 (υC=O), 1622 (υC=N), 1243 (υC=S). Anal. Calcd. for $C_{13}H_{17}N_3OS$: C, 59.29; H, 6.51; N, 15.96. Found: C, 59.57; H, 6.24; N, 16.19.

2.1.8. 3-Benzyl-2-(2-((2,6,6-trimethylcyclohexa-1,3-dienyl) methylene)hydrazono)thiazolidin-4-one (**8**)

The thiazolidinone **7** (1 eq) was suspended in 50 mL of anhydrous acetone in the presence of anhydrous potassium carbonate (1 eq), and reacted with equimolar amounts of benzyl bromide for 48 h at room temperature. The reaction mixture was poured on ice and extracted with chloroform (3 × 50 mL). The organics were reunited, dried over anhydrous sodium sulfate, concentrated *in vacuo* and purified by column chromatography (ethyl acetate:*n*-hexane, 1:2) to give compound **8** as an orange oil (65% yield); ^{1}H NMR (400 MHz, DMSO-d_6): δ 1.18 (s, 6H, 2 × CH_3), 1.96 (s, 3H, CH_3), 2.11–2.12 (m, 2H, CH_2), 4.02 (s, 2H, CH_2-thiazolidinone), 4.90 (s, 2H, CH_2-benzyl), 5.97–6.00 (m, 2H, 2 × CH=), 7.29–7.36 (m, 5H, Ar), 8.36 (s, 1H CH=); ^{13}C NMR (101 MHz, $CDCl_3$) δ 19.45 (CH_3), 26.90 (2 × CH_3), 32.43 (C), 33.74 (CH_2-thiazolidinone), 40.98 (CH_2), 46.56 (CH_2), 127.89 (2 × CH=), 128.48 (2 × CH-benzene), 128.84 (2 × CH-benzene), 129.72 (=CCH_3), 129.98 (C=), 134.22 (CH-benzene), 135.77 (C-benzene), 137.80 (C=N), 157.86 (C=N-thiazolidinone), 172.14 (C=O); IR (neat): cm^{-1} 1722 (υC=O), 1601 (υC=N). Anal. Calcd. for $C_{20}H_{23}N_3OS$: C, 67.96; H, 6.56; N, 11.89. Found: C, 68.20; H, 6.81; N, 11.53.

2.1.9. 1-(4-(3-Nitrophenyl)thiazol-2-yl)-2-((2,6,6-trimethylcyclohexa-1,3-dienyl)methylene)hydrazine (**9**)

The intermediate thiosemicarbazone **4** (1 eq) reacted with 2-bromo-3'-nitroacetophenone (1 eq) in ethanol (50 mL) at room temperature under magnetic stirring for 24 h. The reaction mixture was concentrated *in vacuo*, and the resulting solid was purified by column chromatography (ethyl acetate:light petroleum, 1:2) to give product **9** as a brown powder (mp 120–125 °C, 87% yield); ^{1}H NMR (400 MHz, DMSO-d_6): δ 1.09 (s, 3H, CH_3), 1.21 (s, 3H, CH_3), 1.93 (s, 3H, CH_3), 2.10–2.12 (m, 2H, CH_2), 5.92–5.94 (m, 2H, 2 × CH=), 7.59 (s, 1H, C_5H-thiazole), 7.70–7.80 (m, 1H, Ar), 8.04 (s, 1H, Ar), 8.13–8.22 (m, 1H, Ar), 8.27–8.33 (m, 1H, Ar), 8.66 (s, 1H, CH=), 11.91 (bs, 1H, NH, D_2O exch.); ^{13}C NMR (101 MHz, DMSO-d_6) δ 15.59 (CH_3), 27.16 (2 × CH_3), 33.52 (C), 107.02 (C_5H-thiazole), 120.53 (CH-benzene), 122.15 (CH-benzene), 130.51 (2 × CH=), 130.58 (CH-benzene), 131.95 (CH-benzene), 133.43 (C-benzene), 139.62 (=CCH_3), 141.50 (C=), 145.25 (C=N), 148.67 (C_4-thiazole), 148.89 (C-benzene), 170.03 (C_2-thiazole), (CH_2 signal missing due to overlap with DMSO-d_6); IR (neat): cm^{-1} 1531 (υ_{as} N–O), 1347 (υ_s N–O). Anal. Calcd. for $C_{19}H_{20}N_4O_2S$: C, 61.94; H, 5.47; N, 15.21. Found: C, 62.22; H, 5.19; N, 14.98.

2.2. hMAO inhibition studies

As enzyme sources, commercially available (Sigma–Aldrich, Milan, Italy) microsomes from insect cells, containing recombinant hMAO-A and hMAO-B, were employed. The enzyme activity measurements were based on the hMAO-A or hMAO-B catalyzed oxidation of kynuramine to 4-hydroxyquinoline. The incubations were conducted in 500 μL potassium phosphate buffer (100 mM, pH 7.4, made isotonic with KCl 20.2 mM) in the presence of various concentrations of the test inhibitors and 4% DMSO as the cosolvent. For hMAO-A activity measurements the reactions contained 45 μM kynuramine while for the for hMAO-B activity measurements the kynuramine concentration was 30 μM. The reactions were initiated with the addition of hMAO-A or hMAO-B (0.0075 mg protein/mL) and, following a 20 min incubation at 37 °C, the reactions were terminated by the addition of 400 μL NaOH (2 N) and 1000 μL water. The concentrations of 4-hydroxyquinoline were subsequently measured spectrofluorometrically at excitation and emission wavelengths of 310 nm and 400 nm, respectively (Varian Cary Eclipse fluorescence spectrophotometer). Quantitative estimations of 4-hydroxyquinoline were made with a linear calibration curve constructed with known amounts (0.047–1.56 μM) of the authentic metabolite. The necessary control samples were included to confirm that the test inhibitors do not fluoresce or quench the fluorescence of 4-hydroxyquinoline under these assay conditions. IC_{50} values were calculated by plotting the initial rate of kynuramine oxidation versus the logarithm of the inhibitor concentration to obtain a sigmoidal dose–response curve. For this purpose, the kinetic data were fitted to the one site competition model incorporated into the Prism 5 software package (GraphPad). The IC_{50} values are reported as the mean ± standard deviation (SD) of triplicate determinations (Table 1).

2.3. In silico methods

The X-ray coordinates of hMAO-A and hMAO-B, in complex with harmine and safinamide, respectively, were extracted from the PDB [26], codes 2Z5X [27] and 2V5Z [28]. The protein structures were prepared using the Protein Preparation Wizard [29] of the graphical user interface of Maestro 9.4 [30]. *In silico* experiments were performed with selected ligands, among which are compounds which exhibited potent hMAO inhibition (Table 1). The compounds selected for the *in silico* study were: crocin **1**, semicarbazone **3**, thiosemicarbazone **4** and hydrazothiazole **9**. In particular, the modeling study proved to be useful to establish that crocin **1** and semicarbazone **3**, which possess similar IC_{50} values for the inhibition of the hMAOs while having very different structures, bind to distinct sites on the hMAO proteins. In addition, the *in silico* study also provided insight into how the isosteric substitution S → O causes a significant increase of the hMAO inhibitory activity of the thiosemicarbazone **4** compared to the semicarbazone **3**. To study the interactions of the hMAO isoforms with the test ligands, all water molecules and non-protein residues (except for the FAD cofactor) were removed, hydrogen atoms were added, and finally, energy minimization was performed until the RMSD of all heavy atoms was within 0.3 Å of the original PDB model.

Docking studies were carried out using the Glide [31] SP software. The maximum number of poses for ligands in the receptor cavity was set to 10. The experiments employed full ligand flexibility in the 3D structures of rigid receptor active sites. The default settings of Glide 5.9 were used for the remaining parameters. For each docking run the binding site was defined as a cube of 25 Å. This cube was centered on the former positions of the removed co-

Table 1
The IC_{50} values for the inhibition of hMAO-A and hMAO-B by compounds **1**–**9**.

Compound	IC_{50} MAO-A (μM)	IC_{50} MAO-B (μM)
1 (crocin)	170 ± 22.4	128 ± 10.9
2 (safranal)	No inhibition	No inhibition
3	164 ± 12.8	111 ± 6.26
4	56.8 ± 2.59	74.5 ± 5.68
5	93.2 ± 3.07	117 ± 12.7
6	19.5 ± 2.65	224 ± 30.7
7	132 ± 8.59	168 ± 6.90
8	86.6 ± 5.25	215 ± 16.5
9	9.93 ± 1.51	0.100 ± 0.010

crystallized ligands in the active sites. The natural (**1**) and semisynthetic compounds (**3**, **4** and **9**) were prepared by the LigPrep [32] module, taking into account additional protonated and tautomeric forms calculated at pH 5–9. In order to verify the docking precision of Glide SP, harmine and safinamide were redocked into the hMAO active sites. The docking protocol possessed the ability to reproduce the binding modes of harmine and safinamide, with a very low RMSD values between the ligand position in the experimental X-ray structure and the best docked pose (harmine: 0.08 Å; safinamide: 0.16 Å). After each docking simulation, a positive result was gained when the G-score of the ligand was better than the respective X-ray G-score, with a tolerance of ±10%.

With this experimental protocol, crocin (**1**), due to steric hindrance, is unable to fit into the active sites of hMAO-A and hMAO-B. It was thus decided to perform a blind-docking procedure which allows for binding to alternative pockets with allosteric functions. For this ligand, the site partitioning approach was followed to sample different parts of the binding cavity. In the second phase, docking between the receptor and ligand was performed considering only one specific site for both isoforms. The MM-GBSA method available in Schrödinger Software Prime 3.3 [33] was used to calculate ligand binding and strain energies (MM-GBSA dG Bind). The Pymol 1.5.0.4 [34] molecular graphics system was used to visualize the results of the docking experiments.

3. Results and discussion

Starting from the commercially available natural product safranal (**2**), which was purified by column chromatography, we designed and synthesized (thio)semicarbazone (**3**–**6**), thiazolidinone (**7**–**8**) and hydrazothiazole (**9**) derivatives. For these derivatives, the safranal nucleus was retained in order to evaluate the effects of an increasing steric hindrance and different substituents on hMAO inhibition potency. The general approach for the synthesis of these derivatives is outlined in Scheme 1. Safranal was reacted in ethanol with semicarbazide, thiosemicarbazide, 2-methylthiosemicarbazide and 4-phenylthiosemicarbazide to yield products **3**–**6** [25]. Compound **4** was subsequently reacted with ethyl-bromoacetate in a mixture of methanol and sodium acetate to obtain the 1,3-thiazolidin-4-one derivative **7**. The lactamic nitrogen of thiazolidinone **7** was functionalized using benzyl bromide in anhydrous acetone and potassium carbonate to yield the *N*-benzylated derivative **8**. To obtain the hydrazothiazole **9**, thiosemicarbazone **4** was reacted with 2-bromo-3'-nitroacetophenone in ethanol. All the synthesized compounds were washed with *n*-hexane and light petroleum and purified by column chromatography before characterization by spectroscopic methods and elemental analysis.

The hMAO inhibitory properties of derivatives **1**–**9** (Table 1) were investigated using commercially available microsomes from insect cells containing recombinant hMAO-A and hMAO-B with kynuramine as the substrate [35].

The results of the hMAO inhibition experiments show that the natural product crocin (**1**) display IC_{50} values in the higher micromolar range for the inhibition of hMAO-A and hMAO-B (170 μM and 128 μM, respectively). Crocin is therefore a relatively weak inhibitor of the hMAOs, and unless high brain levels are attained after the administration of saffron extracts to humans and experimental animals, the inhibition of the hMAOs is unlikely to represent a mechanism by which saffron extracts confer antidepressant and neuroprotective effects. Further investigation into the *in vivo* MAO inhibitory properties, the pharmacokinetic properties and in particularly brain tissue levels of crocin, are necessary to completely elucidate the contribution of crocin to the neuropharmacological actions of saffron extracts. Safranal (**2**), the major component of the volatile fraction of saffron, did not show any inhibition of the hMAO isoforms. In contrast, the semisynthetic derivatives of safranal possess interesting biological properties. For example, although relatively weak inhibitors, both semicarbazone **3** [IC_{50}(MAO-A) = 164 μM; IC_{50}(MAO-B) = 111 μM] and thiazolidinone **7** [IC_{50}(MAO-A) = 132 μM; IC_{50}(MAO-B) = 168 μM] were found to be inhibitors of hMAO-A and hMAO-B. Similarly, 2-methylthiosemicarbazone derivative **5** [IC_{50}(MAO-A) = 93.2 μM; IC_{50}(MAO-B) = 117 μM] and *N*-benzylated thiazolidinone **8** [IC_{50}(MAO-A) = 86.6 μM; IC_{50}(MAO-B) = 215 μM] also proved to be relatively weak inhibitors of hMAO-A and hMAO-B. Thiosemicarbazone **4** possessed higher potencies for the inhibition of hMAO-A and hMAO-B with IC_{50} values of 56.8 μM and 74.5 μM, respectively. Interestingly, 4-phenylthiosemicarbazone **6** was found to be a moderately potent hMAO-A inhibitor with an IC_{50} value of 19.5 μM. This compound also represents a relatively selective hMAO-A inhibitor since it is 11-fold more potent as a hMAO-A inhibitor compared to its hMAO-B inhibition potency [IC_{50}(MAO-B) = 224 μM]. The most notable inhibitor of the series, however, is the hydrazothiazole derivative **9**, which is the most potent inhibitor of both hMAO-A and hMAO-B among the compounds evaluated. In fact, **9** is a highly potent hMAO-B inhibitor with an IC_{50} value of 0.100 μM. Even though **9** also is a notable hMAO-A inhibitor [IC_{50}(hMAO-A) = 9.93 μM], it is 99-fold more potent as a hMAO-B inhibitor, and thus the most isoform selective inhibitor of the series. For comparison, the reversible hMAO-A inhibitor, toloxatone, is reported to inhibit hMAO-A with an IC_{50} value of 3.92 μM, while the well known reference hMAO-B inhibitor lazabemide exhibits an IC_{50} of 0.091 μM for the inhibition of hMAO-B [36]. The IC_{50} value for the inhibition of hMAO-B recorded for compound **9** is 0.100 μM, a value that is similar to the reported IC_{50} value for the inhibition of hMAO-B by lazabemide. Compound **9** is therefore approximately equipotent to lazabemide as a hMAO-B inhibitor. Although no clear structure–activity relationships are apparent, this study shows that, with the appropriate substitution, the structure of safranal may be converted into highly potent hMAO-B inhibitors, and moderately potent hMAO-A inhibitors. In this respect, compound **9** is a highly promising and novel scaffold for the design of future hMAO inhibitors. Further structural modification of **9** should be undertaken to derive useful structure–activity relationships for the inhibition of the hMAOs by this class of inhibitors, and to further optimize the structure for potent and selective hMAO inhibition.

During *in silico* molecular docking studies, the goal is to establish the general binding orientations of the ligands, to determine the nature of the interactions between the ligands and receptor and to estimate affinities of the ligands for the receptor by calculating binding energies. Stabilization of ligands is mainly attributed to the formation of productive contacts between ligands and the target protein. For the binding of **1**, **3**, **4** and **9** to hMAO-A and hMAO-B, these contacts are given in Table S1 of Supporting Information.

4. Mechanism of action

In this study, the binding of crocin (**1**) and safranal derivatives **3**, **4** and **9** to the hMAO enzymes were examined. The global energy of interactions (in kcal/mol) for each docking experiment is reported in Table S2 (Supporting Information). As will be discussed below, derivatives **3**, **4** and **9** fit within the active site cavities of the hMAOs with acceptable G-score values (<X-ray G-score). Since crocin (**1**) does not fit within the active sites of hMAO-A and hMAO-B, a blind-docking simulation was carried out and a potential allosteric site where crocin may bind was identified. This site is situated in the area near the gate of the entrance tunnel to the binding pocket.

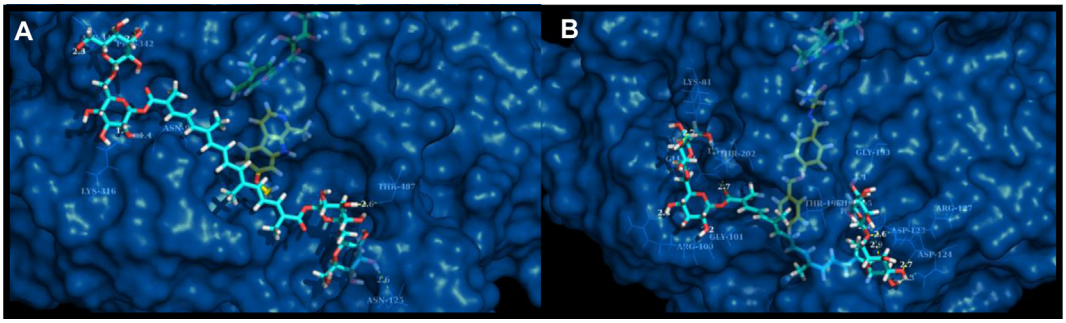

Fig. 1. (A) Best pose of crocin (**1**) and its polar contacts with respective distances on the hMAO-A surface. The natural ligand is rendered as cyan sticks, pocket amino acids are shown as blue lines, the superimposed reference drug (harmine) as yellow sticks, FAD co-factor is highlighted with green sticks, while the protein target is shown as a blue surface. All molecules are colored according to atom type. (B) Best pose of crocin (**1**) and its polar contacts with respective distances on the hMAO-B surface. The natural ligand is rendered as cyan sticks, pocket amino acids are shown as blue lines, the superimposed reference drug (safinamide) as yellow sticks, the FAD co-factor is highlighted with green sticks, while the protein target is shown as a blue surface. All molecules are colored according to atom type. (For interpretation of the references to color in this figure legend, the reader is referred to the web version of this article.)

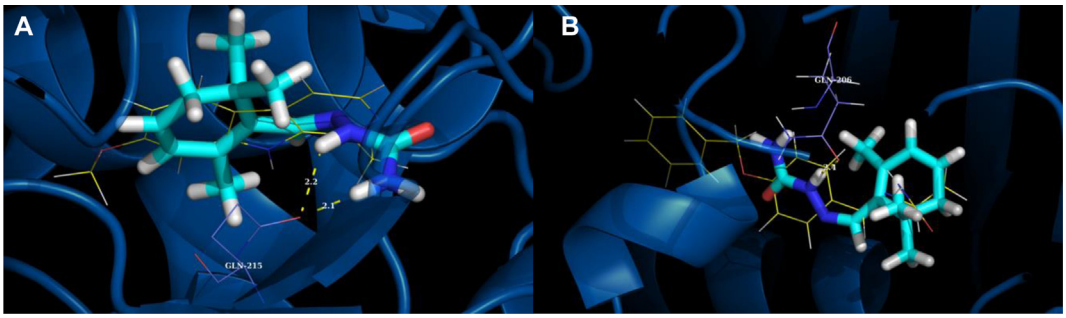

Fig. 2. (A) Semicarbazone **3** best pose and its polar contacts with respective distances in the hMAO-A binding cavity. The ligand is rendered as cyan sticks, the GLN215 pocket amino acid is shown as blue lines, the superimposed reference drug (harmine) as yellow lines, and the protein target is shown as a blue cartoon. All molecules are colored according to atom type. (B) Semicarbazone **3** best pose and its polar contacts with respective distances in the hMAO-B binding cavity. The ligand is rendered as cyan sticks, the GLN206 pocket amino acid is shown as blue lines, the superimposed reference drug (safinamide) as yellow lines, and the protein target is shown as a blue cartoon. All molecules are colored according to atom type. (For interpretation of the references to color in this figure legend, the reader is referred to the web version of this article.)

A computational study, carried out following our recently published protocol [37,38], reveals that crocin (**1**) inhibits both hMAO isoforms with a non-competitive mechanism of action. As shown in Fig. 1, crocin does not fit into the binding pocket of either hMAO-A or hMAO-B. The modeling study suggests that crocin binds to the protein surface, to an allosteric site, and may thus inhibit the catalysis of amine substrates. In agreement with the *in vitro* inhibition data, which shows that crocin is a more potent hMAO-B inhibitor, crocin better interacts with the hMAO-B than the hMAO-A isoform, as shown by the MM-GBSA dG Bind values (Table S2), and by the higher number of interactions (H-bonds) which it establishes with the amino acids, to stabilize the pose (Fig. 1 and Table S1 of the Supporting Information). In the case of isoform A, in its best pose, crocin fits well on the target surface, blocking with its central portion the access to the active site; in the case of hMAO-B isoform, a part of the natural ligand is placed into a cavity on the surface. In both poses, H-bonds interactions occur between the polar OH groups located at the terminal ends of crocin and enzyme surface residues.

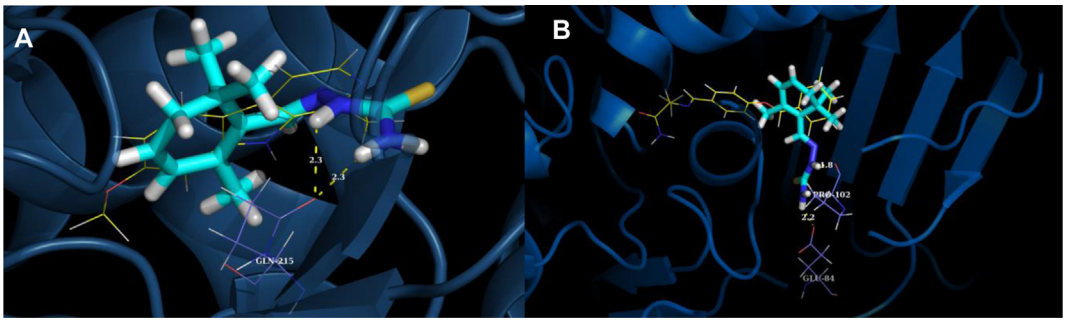

Fig. 3. (A) Thiosemicarbazone **4** best pose and its polar contacts with respective distances in the hMAO-A binding site. The ligand is rendered as cyan sticks, the GLN215 pocket amino acid is shown as blue lines, the superimposed reference drug (harmine) as yellow lines, and the protein target is shown as a blue cartoon. All molecules are colored according to atom type. (B) Thiosemicarbazone **4** best pose and its polar contacts with respective distances in the hMAO-B binding cavity. The ligand is rendered as cyan sticks, the GLU84 and PRO102 pocket amino acids are shown as blue lines, the superimposed reference drug (safinamide) as yellow lines, and the protein target is shown as a blue cartoon. All molecules are colored according to atom type. (For interpretation of the references to color in this figure legend, the reader is referred to the web version of this article.)

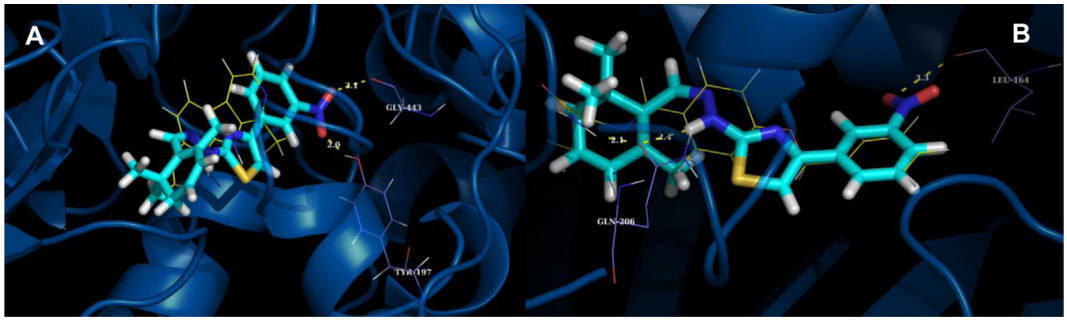

Fig. 4. (A) Best pose of hydrazothiazole **9** and its polar contacts with respective distances in the hMAO-A binding cavity. The ligand is rendered as cyan sticks, the TYR197 and GLY443 pocket amino acids are shown as blue lines, the superimposed reference drug (harmine) as yellow lines, and the protein target is shown as a blue cartoon. All molecules are colored according to atom type. (B) Best pose of hydrazothiazole **9** and its polar contacts with respective distances in the hMAO-B binding cavity. The ligand is rendered as cyan sticks, the LEU164 and GLN206 pocket amino acids are shown as blue lines, the superimposed reference drug (safinamide) as yellow lines, while the protein target is shown as a blue cartoon. All molecules are colored according to atom type. (For interpretation of the references to color in this figure legend, the reader is referred to the web version of this article.)

Despite the similar values of the hMAO inhibition potencies of crocin and the semicarbazone derivative **3**, computational studies suggest that **3** may act as a competitive inhibitor, with its best pose located in the binding pocket (Fig. 2). In accordance to the hMAO inhibition data (IC_{50} values in Table 1), the G-score values obtained in the docking simulations (Table S2) also show that thiosemicarbazone **4** is a more potent hMAO inhibitor than is semicarbazone **3**. While the isosteric substitution S → O does not affect the general binding orientation of **4** within hMAO-A (compared to **3**) and the H-bond interaction with GLN215 in hMAO-A, it results in significantly different interactions of **4** with hMAO-B compared to the interactions observed between **3** and hMAO-B (Fig. 3).

Finally, based on the G-score values, hydrazothiazole **9** is a more potent hMAO-B inhibitor than compounds **3** and **4**, an observation supported by the hMAO inhibition data. The docking simulation further shows that **9** binds within the hMAO-B active site, and is therefore most likely a competitive inhibitor. Interestingly, the G-score values calculated for binding of **9** to hMAO-A and hMAO-B suggest that this compound is a selective inhibitor of the hMAO-B isoform, which is in accordance to the results of the hMAO inhibition studies (Fig. 4).

5. Conclusion

A variety of studies have suggested that saffron may have a potential role in the treatment of mental disorders such as depression, or may enhance the beneficial effects of conventional drugs with fewer side effects. Based on this consideration, we investigated the hMAO-A and hMAO-B inhibitory properties of two natural components of *C. sativus* L., crocin (**1**) and safranal (**2**), as well as those of newly designed compounds (**3**–**9**) derived from chemical modifications of safranal. hMAO-A and hMAO-B are two important enzymes which are targets for the treatment of neuropsychiatric and neurodegenerative diseases. The results document that, while crocin is a relatively weak inhibitor of the hMAOs, safranal is not a hMAO inhibitor. Based on this, we conclude that the inhibition of the MAOs by crocin and safranal are unlikely to represent mechanisms by which saffron extracts confer their beneficial central effects. The designed chemical derivatives of safranal, however, displayed much improved inhibitory activities against both hMAO enzymes. In this respect, compound **9** was found to be an exceptionally potent hMAO-B inhibitor, and thus a highly promising and novel scaffold for the design of future hMAO-B inhibitors. Compound **9** also displayed relatively good selectivity for the hMAO-B isoform. Further structural modification of **9** should be undertaken to derive more useful structure–activity relationships for the inhibition of the hMAOs by this promising class of compounds, and possibly to further enhance isoform selectivity.

Molecular docking studies were carried out on natural crocin (**1**) and the semisynthetic compounds **3**, **4** and **9**. The results suggest that crocin may inhibit both hMAO isoform with non-competitive mechanisms by binding to allosteric sites on the surfaces of the proteins. In contrast, the semisynthetic compounds **3**, **4** and **9** bind within the active sites of the hMAOs and may thus act competitively. The results of the docking studies were also in agreement with the finding that thiosemicarbazone **4** is a more potent hMAO inhibitor than semicarbazone **3**, and that hydrazothiazole **9** acts as a selective inhibitor of the hMAO-B enzyme. The results of this study show that, with the appropriate chemical modification, safranal may serve as scaffold for the discovery of hMAO inhibitors for the clinical management of mental and neurodegenerative disorders.

Conflict of interest

The authors state no conflict of interest and that they have received no payment in preparation of this manuscript.

Acknowledgments

This work was supported by "Ateneo 2012" project (P. Chimenti and L. Mannina) using the facilities of the "Unit of Metabolomics: Studies on Food, Nutraceuticals and Biological Fluids" and by Interregional Research Center for Food Safety and Health at the Magna Græcia University of Catanzaro (MIUR PON a3_00359).

Appendix A. Supplementary data

Supplementary data related to this article can be found at http://dx.doi.org/10.1016/j.ejmech.2014.05.048.

References

[1] (a) S. Carradori, M. D'Ascenzio, P. Chimenti, D. Secci, A. Bolasco, Mol. Divers. 18 (2014) 219–243;
(b) S. Carradori, D. Secci, A. Bolasco, P. Chimenti, M. D'Ascenzio, Expert Opin. Ther. Patents 22 (2012) 759–801;
(c) A. Bolasco, R. Fioravanti, S. Carradori, Expert Opin. Ther. Patents 15 (2005) 1763–1782;
(d) A. Bolasco, S. Carradori, R. Fioravanti, Expert Opin. Ther. Patents 20 (2010) 909–939.
[2] J. Sarris, A. Panossian, I. Schweitzer, C. Stough, A. Scholey, Eur. Neuropsychopharmacol. 21 (2011) 841–860.

[3] S.Z. Bathaie, S.Z. Mousavi, Crit. Rev. Food Sci. Nutr. 50 (2010) 761–786.
[4] B.A. Wani, A.K.R. Hamza, F.A.J. Mohiddin, Med. Plant. Res. 5 (2011) 2131–2135.
[5] Z.I. Linardaki, M.G. Orkoula, A.G. Kokkosis, F.N. Lamari, M. Margarity, Food Chem. Toxicol. 52 (2013) 163–170.
[6] M. Lechtenberg, D. Schepmann, M. Niehues, N. Hellenbrand, B. Wünsch, A. Hensel, Planta Med. 74 (2008) 764–772.
[7] A.A. Basti, E. Moshiri, A.A. Noorbala, A.H. Jamshidi, S.H. Abbasi, S. Akhondzadeh, Prog. Neuro-psychopharmacol. Biol. Psychiatry 31 (2007) 439–442.
[8] A.A. Noorbalaa, S. Akhondzadeh, N. Tahmacebi-Pour, A.H. Jamshidi, J. Ethnopharmacol. 97 (2005) 281–284.
[9] S. Akhondzadeh, H. Fallah-Pour, K. Afkham, A.H. Jamshidi, F. Khalighi-Cigaroudi, BMC Complement. Altern. Med. 4 (2004) 12–16.
[10] E. Moshiria, A.A. Bastib, A.A. Noorbalac, A.H. Jamshidid, S.H. Abbasie, S. Akhondzadehc, Phytomedicine 13 (2006) 607–611.
[11] L. Kashani, F. Raisi, S. Saroukhani, H. Sohrabi, A. Modabbernia, A.-A. Nasehi, A. Jamshidi, M. Ashrafi, P. Mansouri, P. Ghaeli, S. Akhondzadeh, Hum. Psychopharmacol. Clin. Exp. 28 (2013) 54–60.
[12] A. Modabbernia, H. Sohrabi, A.-A. Nasehi, F. Raisi, S. Saroukhani, A. Jamshidi, M. Tabrizi, M. Ashrafi, S. Akhondzadeh, Psychopharmacology 223 (2012) 381–388.
[13] M. Schmidt, G. Betti, A. Hensel, Wien. Med. Wochenschr. 157 (2007) 315–319.
[14] G. Georgiadoua, P.A. Tarantilis, N. Pitsikas, Neurosci. Lett. 528 (2012) 27–30.
[15] F. Di Marco, S. Romeo, C. Nandasena, S. Purushothuman, C. Adams, S. Bisti, J. Stone, Am. J. Neurodegener. Dis. 2 (2013) 208–220.
[16] M.A. Papandreou, C.D. Kanakis, M.G. Polissiou, S. Efthimiopoulos, P. Cordopatis, M. Margarity, F.N. Lamari, J. Agric. Food Chem. 54 (2006) 8762–8768.
[17] G.D. Geromichalos, F.N. Lamari, M.A. Papandreou, D.T. Trafalis, M. Margarity, A. Papageorgiou, Z. Sinakos, J. Agric. Food Chem. 60 (2012) 6131–6138.
[18] K.N. Westlund, R.M. Denney, R.M. Rose, C.W. Abell, Neuroscience 25 (1988) 439–456.
[19] D.E. Edmondson, C. Binda, J. Wang, A.K. Upadhayay, A. Mattevi, Biochemistry 48 (2009) 4220–4230.
[20] M.B.H. Youdim, D.E. Edmondson, K.F. Tipton, Nat. Rev. 7 (2006) 295–309.
[21] M. Bortolato, K. Chen, J.C. Shih, Adv. Drug. Deliv. Rev. 60 (2008) 1527–1533.
[22] (a) S. Carradori, M. D'Ascenzio, C. De Monte, D. Secci, M. Yáñez, Arch. Pharm. Chem. Life Sci. 346 (2013) 17–22;
(b) M. D'Ascenzio, S. Carradori, D. Secci, L. Mannina, A.P. Sobolev, C. De Monte, R. Cirilli, M. Yáñez, S. Alcaro, F. Ortuso, Bioorg. Med. Chem. 22 (2014) 2887–2895.
[23] (a) P. Chimenti, A. Petzer, S. Carradori, M. D'Ascenzio, R. Silvestri, S. Alcaro, F. Ortuso, J.P. Petzer, D. Secci, Eur. J. Med. Chem. 66 (2013) 221–227;
(b) S. Carradori, D. Secci, P. D'Ascenzio, A. Bolasco, J. Heterocycl. Chem. (2014), http://dx.doi.org/10.1002/jhet.1856.
[24] D. Secci, A. Bolasco, S. Carradori, M. D'Ascenzio, R. Nescatelli, M. Yáñez, Eur. J. Med. Chem. 58 (2012) 405–417.
[25] F. Chimenti, D. Secci, A. Bolasco, P. Chimenti, A. Granese, S. Carradori, M. Yáñez, F. Orallo, F. Ortuso, S. Alcaro, Bioorg. Med. Chem. 18 (2010) 5715–5723.
[26] H.M. Berman, J. Westbrook, Z. Feng, G. Gilliland, T.N. Bhat, H. Weissig, I.N. Shindyalov, P.E. Bourne, Nucleic Acids Res. 28 (2000) 235–242.
[27] S.Y. Son, J. Ma, Y. Kondou, M. Yoshimura, E. Yamashita, T. Tsukihara, Proc. Natl. Acad. Sci. U. S. A. 105 (2008) 5739–5744.
[28] C. Binda, J. Wang, L. Pisani, C. Caccia, A. Carotti, P. Salvati, D.E. Edmondson, A. Mattevi, J. Med. Chem. 50 (2007) 5848–5852.
[29] Schrödinger Suite 2013 Protein Preparation Wizard; Epik Version 2.4, Schrödinger, LLC, N. Y. N. Y., 2013; Impact Version 5.9, Schrödinger, LLC, New York, NY, 2013; Prime Version 3.2, Schrödinger, LLC, New York, NY, 2013.
[30] Maestro, Version 9.4, Schrödinger, LLC, New York, NY, 2013.
[31] Glide, Version 5.9, Schrödinger, LLC, New York, NY, 2013.
[32] LigPrep, Version 2.6, Schrödinger, LLC, New York, NY, 2013.
[33] Prime, Version 3.3, Schrödinger, LLC, New York, NY, 2013.
[34] The PyMOL Molecular Graphics System, Version 1.5.0.4 Schrödinger, LLC.
[35] L. Novaroli, M. Reist, E. Favre, A. Carotti, M. Catto, P.-A. Carrupt, Bioorg. Med. Chem. 13 (2005) 6212–6217.
[36] A. Petzer, A. Pienaar, J.P. Petzer, Drug Res. 63 (2013) 462–467.
[37] F. Chimenti, R. Fioravanti, A. Bolasco, F. Manna, P. Chimenti, D. Secci, O. Befani, P. Turini, F. Ortuso, S. Alcaro, J. Med. Chem. 50 (2007) 425–428.
[38] A. Gaspar, T. Silva, M. Yáñez, D. Vina, F. Orallo, F. Ortuso, E. Uriarte, S. Alcaro, F. Borges, J. Med. Chem. 54 (2011) 5165–5173.